PHYSICAL REVIEW E **76**, 040701(R) (2007)

Carrier transport simulation of anomalous temperature dependence in nematic liquid crystals

Masanao Goto,* Hideo Takezoe, and Ken Ishikawa
Department of Organic and Polymeric Materials, Tokyo Institute of Technology, O-Okayama, Meguro-ku, Tokyo, 152-8552, Japan
(Received 8 June 2007; published 1 October 2007)

We investigated the carrier transport phenomena in model liquid crystalline systems, which were constructed on the basis of the Gay-Berne potential and Monte Carlo calculation. The carrier transport was analyzed under the condition that the molecular arrangement in the system was fixed and thermally activated carriers were transported by hopping in the system. The carrier transport simulation was performed by Monte Carlo method using Miller-Abrahams hopping ratio. By these calculations, we reproduced the experimental results of the electronic conduction in nematic liquid crystals.

DOI: 10.1103/PhysRevE.76.040701 PACS number(s): 61.30.Cz, 64.70.Md, 72.20.Ee

I. INTRODUCTION

The liquid crystalline semiconductors have received much attention because of their potential application for organic electronic devices. Owing to intensive studies, the carrier mobility in liquid crystal phases has reached a comparable level with that of the crystalline materials [1–3]. For calamitic liquid crystals, electronic transport had been confirmed only in smectic phases and had never been observed in fluidic phases like the nematic phase. However, the electronic transport in the nematic phase, showing a characteristic temperature dependence of the carrier mobility, was recently reported by several groups [4–6].

The carrier transport in liquid crystals is generally understood by uncorrelative hopping transport in a lattice system like the Gaussian disorder model [7] or other modified models [8–10]. These models sufficiently explain the experimental results in the discotic [11] and smectic [12] phases in which the mobility scarcely depends on temperature and electric field. However the situation is more complicated in the nematic phase. The mobility gradually increases with cooling in the nematic phase [5,6]. The sign inversion of the temperature dependence at the nematic-isotropic phase transition point is also observed in some molecules [5]. It would be difficult to explain these temperature dependencies in the framework of the Gaussian disorder model with temperature-independent parameters σ and Σ representing the energetic and positional disorder, respectively. It is possible to explain these temperature dependencies by introducing some temperature dependence to these parameters, but we have little insight about the relationship between the molecular order and these parameters.

In this paper, we investigate hopping carrier transport in a model liquid crystalline system to clarify the origin of the distinctive temperature dependence of the mobility in the nematic phase. For this purpose, we simulated molecular arrangement of a Gay-Berne fluid composed of spheroid particles. Subsequently, we examined the hopping transport among these particles using the Miller-Abrahams hopping rate. The electronic potential of each hopping site was determined by two methods, which is distinguished by the spatial distribution of disorder, resulting in different temperature dependence of the mobility.

II. METHOD

Despite of the amazing improvement of computing power, the molecular simulation based on an atomistic model is still difficult particularly for the nematic phase, because a large simulation box is necessary to represent the nematic phase without periodicity. Thus there have been only a few reports dealing with atomistic models of the nematic phase [13,14]. Additionally, atomistic models only give the information about a specific molecule, while we want to elucidate the fundamental mechanism of the electronic transport in the nematic phase. Therefore, we chose a simple spheroid shape model with Gay-Berne potential [15–18] in this simulation.

We followed the simulation method described in reference [18] to obtain the molecular arrangement. We performed the Monte Carlo simulation using the Gay-Berne potential. The shape of each molecules was set to spheroid whose lengths of the major and minor axes were $3\sigma_0$ and σ_0, respectively, where σ_0 is the unit length in this simulation. For the interaction of the molecules we only took into account the short-ranged molecular interactions calculated by the Gay-Berne potential and ignored electrostatic interactions. The parameters were chosen to be the same as the uniaxial case of Ref. [18].

The simulation was done by N-P-T ensemble with $N=1024$ particles. Pressure and temperature were specified as dimensionless parameters $P^*=\sigma_0^3 P/\epsilon_0$ and $T^*=kT/\epsilon_0$ respectively, where ϵ_0 is the unit energy of the Gay-Berne potential, P is the pressure, T is the temperature, and k is the Boltzmann constant. We employed a rectangular box with periodic boundary conditions. Each length of the box was independently changed in each Monte Carlo step. Therefore, a Monte Carlo step (mcs) consisted of two parts, trial movement of each particle and trial change of the box size. In a trial movement of each particle, we changed position and orientation of a spheroid at the same time. The maximum changes of the trial were adjusted during the simulation runs so that the acceptances of the trial movement and the trial volume change were kept to be 0.4 and 0.1, respectively.

Contrary to the Ref. [18] we often obtained some unrealistic phases in which the molecular directions were not

*gmasanao@mbox.op.titech.ac.jp

aligned while the positions were placed as a crystal in cooling sequence. Therefore, each simulation run was started from the crystal state in the low temperature. Then the system was heated up to desired temperatures with fixed pressure $P^*=8.0$. To obtain the equilibrium configurations at each temperature, 30 000 Monte Carlo cycles (mcs) were typically used. After attaining the equilibrium configuration, 10 000 mcs were performed and averaged over 500 times by taking one datum per every 20 mcs to obtain thermodynamic observables at each temperature.

The average energy per particle $\langle U^* \rangle$ was defined as $\langle U^* \rangle = (1/N)\Sigma_{i,j} U_{ij}^*$. The density ρ^* was defined as $\rho^* = N/V^*$. The nematic order parameter $\langle P_2 \rangle$ was calculated from the largest eigenvalue of the second-order tensor order parameter $Q_{\alpha\beta}$, which was defined as $Q_{\alpha\beta} = (1/N)\Sigma_i \left(\frac{3}{2} n_{i\alpha} n_{i\beta} - \frac{1}{2}\delta_{\alpha\beta}\right)$, where $\alpha, \beta = x, y, z$ and $n_{i\alpha}$ means α component of the unit vector parallel to the long axis of the ith molecule.

Subsequently the carrier transport in the calculated configurations was investigated. We performed the Monte Carlo simulation using Miller-Abrahams type hopping ratio which was established in lattice systems [7]. Hereby we applied this method to a lattice-free system. Initially carriers were randomly distributed to molecules in the initial unit cell, and carriers were transported by hopping in the periodically iterated unit cells under an electric field. Each hopping process consisted of two steps. First, a carrier chose a molecule within some cutoff radius r_{hop}. Then the carrier hopped onto the molecule with the Miller-Abrahams type hopping rate. In other words, the acceptance v of the hopping within some time period Δt was given as follows:

$$v = v_0 \Delta t \exp\left(\frac{r_{ij}}{r_0}\right) \min\left[1, \exp\left(-\frac{\epsilon_j - \epsilon_i}{kT}\right)\right], \tag{1}$$

where v_0 is the hopping frequency, r_{ij} is the distance between ith and jth molecules, r_0 is the decay length of the transfer integral, and ϵ_i is the potential of the ith molecule modified by the applied electric field. Any interections between carriers were ignored. For obtaining the transit time, two parallel planes, the start and the end ones, with the distance of L were placed perpendicular to the electric field. The origin of the initial unit cell was on the start plane. During the simulation, carriers moving backward and crossing out of the start plane were removed. In addition, carriers moving forward and crossing out of the end plane were also removed, and the time was recorded as the transit time of them. After iterating this hopping process with all carriers, the system time was advanced by Δt. This process was repeated until all carriers had been removed.

The electronic potential of each hopping site was calculated by two methods. In the Gaussian method the Gaussian distribution with standard deviation s^* was used. In the dipole method, the potential of each molecule was calculated from the permanent dipoles of surrounding molecules. A dipole parallel to one of the short axes was placed at the center of a molecule. Each dipole was treated as a closely separated pair of charges. The separation length was set to $0.02\sigma_0$. The electrostatic potential at the center of each molecule was calculated by the Wolf method [19,20] using the cutoff radius $R_c = 5.0\sigma_0$ and the decay coefficient $\alpha = 0.1/\sigma_0$.

Miscellaneous parameters for carrier transport simulation were as follows. The decay length of the molecular overlap r_0 was 0.3. The hopping cutoff radius r_{hop} was 5. The time step Δt was determined to satisfy $v_0 \Delta t \exp(-r_{ij,\min}/r_0) \leqslant 0.5$, i.e., the acceptance of each hopping does not exceed 0.5. In this equation $r_{ij,\min}$ was taken as σ_0, because molecules can not approach nearer than the length of their minor axis.

We performed the carrier transport simulation at various temperatures. At each temperature, the simulation with 100 carriers was repeated 30 times after choosing molecular arrangements randomly out of equilibrated configurations at that temperature. Then the mobility was estimated from the distribution of the transit time. The distribution was successfully fitted by a log-normal distribution, and the mobility was calculated from the mean transit time. The log-normal distribution implies that the transport in this system is basically controlled by trap and release.

The resutls are described using reduced values constructed from the unit length σ_0, the unit energy ϵ_0 and the hopping frequency v_0. We summarize all relations between reduced and real values below. Here the symbols with and without asterisk mean reduced and real values, respectively.

$$s = \epsilon_0 s^*, \tag{2}$$

$$t = \frac{t^*}{v_0}, \tag{3}$$

$$E = \frac{\epsilon_0}{\sigma_0 q} E^*, \tag{4}$$

$$\mu = \frac{\sigma_0 v_0 q}{\epsilon_0} \mu^*, \tag{5}$$

$$p = \frac{4\pi\varepsilon\sigma_0^2\epsilon_0}{q} p^*, \tag{6}$$

where s is the standard deviation of the Gaussian distribution, t is the time, E is the applied electric field, μ is the mobility, p is the electric dipole, and ε is the dielectric constant of this system. In this simulation, the dielectric constant was considered as constant with temperatures and we assumed the actual dipole moment p stayed unchanged over various temperatures with fixed reduced dipole moment p^*.

III. RESULTS AND DISCUSSION

First, we will explain the results of the molecular arrangement simulation. Figure 1 is the temperature dependence of the thermodynamic observables. In the heating sequence, we found three phases: The crystal, the nematic, and the isotropic phases. All phase transitions were clearly distinguished by the discontinuous change of the thermodynamic observables shown in Fig. 1. Assignment of each phase was done from the order parameter and the snapshots of the molecular arrangement.

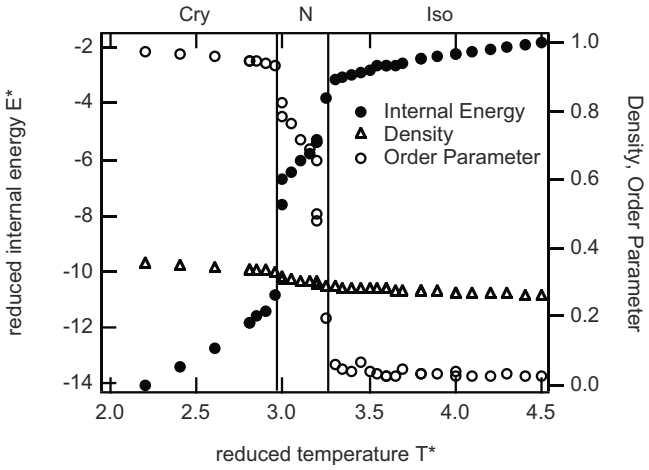

FIG. 1. Temperature dependence of the thermodynamic observables. The system was heated from crystal. Vertical lines indicate the phase boundaries. Cry: Crystal phase; N: Nematic phase; Iso: Isotropic phase. The temperature, the internal energy, and the density are dimensionless values as described in the Method section.

The temperature dependence of the mobility obtained by the Gaussian and the dipole methods at several energetic disorder levels are shown in Figs. 2 and 3, respectively. It is common for both methods that the mobility is anisotropic in the anisotropic phases, i.e., the nematic phase and the crystal phase, and the sign of the anisotropy is the same in both phases. However the anisotropy is smaller in the nematic phase than that in the crystal phase and discontinuously changes at the nematic-crystal phase transition point. The mobility continuously changes at the nematic-isotropic transition while both the internal energy and the order parameter change discontinuously at the transition. A possible explanation is that the simple Miller-Abrahams hopping rate used in this study is affected by the relative position between molecules but little affected by the relative orientation. This nature would make the mobility rather insensitive to the order parameter change.

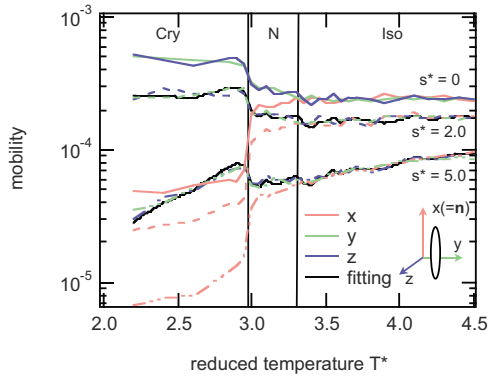

FIG. 2. (Color online) Temperature dependence of the mobility when the disorder is generated by the Gaussian method. The applied electric field E^* is 0.05. The line colors specify the direction of the applied electric field and the resultant current with respect to the director for the mobility measurements. The line types specify the standard deviation of the potential distribution. The black solid lines are the fitting for the perpendicular components for $s^*=2$ and 5. The temperature and the mobility are dimensionless values as described in the Method section.

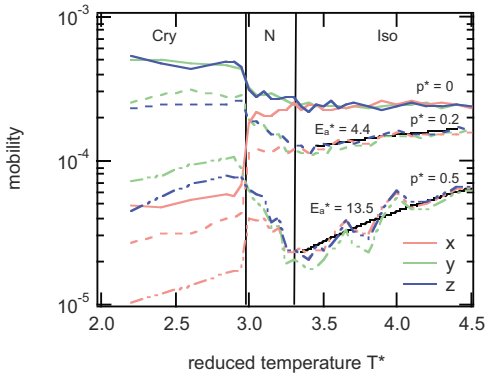

FIG. 3. (Color online) Temperature dependence of the mobility when the disorder was generated by the dipole method. The applied electric field E^* is 0.05. The line colors are the same as in Fig. 2. The line types specify the dipole moment of each molecule which is proportional to the energetic disorder. The black solid lines in the isotropic phase for $p^*=0.2$ and 0.5 are the best fit to the Arrhenius relationship. The temperature and the mobility are dimensionless values as described in the Method section.

Let us discuss the temperature dependence behavior obtained by two methods. In the Gaussian disorder model the temperature dependence of the zero-field mobility is described as $\mu(T)=\mu_0 \exp[-2(\sigma/kT)^2/3]$, where σ is the standard deviation of the potential and is independent of temperature. The temperature dependence obtained by the Gaussian method (Fig. 2) is well fitted by this equation in which μ_0 is replaced by the mobility in a system without disorder ($s^*=0$). We used a temperature-independent multiply $\xi(s^*)$ for the best fit shown by black solid lines in Fig. 2, where only the perpendicular components for $s^*=2$ and 5 are shown. Therefore the mobility at a temperature T^* under a Gaussian distribution with a standard deviation s^* is expressed as

$$\mu(s^*,T^*) = \mu(0,T^*)\xi(s^*)\exp\left[-\frac{2}{3}\left(\frac{\sigma}{kT}\right)^2\right]. \qquad (7)$$

Here, σ is almost equivalent to s^*, since s^* is the reduced standard deviation of the Gaussian distribution.

The temperature dependence of the mobility in the isotropic phase is described by a simple thermal activation type (Arrhenius type), as shown by black solid lines in Fig. 3. This is also the case in the nematic and crystal phases in the results by Gaussian method. For the dipole method (Fig. 3), however, the departure from the simple thermal activation type is found in the nematic phase; the mobility increases with decreasing temperature.

We want to comment on the potential distribution, since the distribution is a key parameter for the simulation. The potential distributions obtained by the dipole method were almost Gaussian, as previously studied [9,10], when the distance between two point charges forming a dipole is sufficiently small. Even if the distribution against energy is the

same, however, the spatial distribution would be quite different; i.e., the long-range spatial correlation exists in the distribution of the disorder derived from the dipole method [9,10], whereas it generally changes much moderately in the Gaussian method. The distribution with $p^*=0.2$ obtained by the dipole model corresponds to the Gaussian distribution with a standard deviation $s^* \simeq 5.52$ at $T^*=4.0$, if the difference in the spatial distributions mentioned above is neglected. In the isotropic phase, the activation energy extracted from the temperature dependence of the dipole method is nearly the same as that corresponding to a standard deviation at $T^*=4.0$. Despite the same distribution, however, the mobility values by the dipole method with $p^*=0.2$ are largely different from those by the Gaussian method with a corresponding standard deviation $s^* \simeq 5.52$, as noticed by comparing the values for $s^*=5.0$ in Fig. 2 and the values for $p^*=0.2$ in Fig. 3. This difference is attributed to the different spatial distribution of the disorder mentioned above. In the nematic phases, the mobility perpendicular to the director does not follow the activation type and gradually increases with decreasing temperature, while the mobility parallel to the director is constant or increases more moderately. It is important to note that the temperature dependence of the mobility perpendicular to the director well simulates an experimental result [5].

The different temperature dependence of the mobility obtained by two methods suggests that the change of the molecular overlap is not the only factor to reproduce the temperature dependence of the mobility in the nematic phase. The disorder derived from the configuration of dipoles is effective to explain experimental results. Actually, the width of the potential distribution derived by the dipoles is not constant against temperature. Especially in the nematic phase, the reduced standard deviations of the potential s^* changes drastically from 21.8 at $T^*=2.9$ to 32.3 at $T^*=3.3$. This change causes the mobility lower in the higher temperature only within the nematic phase and makes the mobility minimum at the isotropic-nematic transition for $p^*=0.5$.

The sign of the anisotropy is the same between the nematic and the crystal phase. The mobility perpendicular to the director is always larger than that along the director. These results in the crystal are consistent to typical electronic conduction in the smectic phases of the calamitic molecules. Since the smectic phases are regarded as a 2D system, the electronic conduction is considered to occur only within the smectic layer. Thus we can predict that the charge carrier mobility along the director is slower than that normal to the director in the actual nematic phase, which is opposite to the mobility of ionic conduction in the nematic phase [21,22].

In conclusion, we succeeded in replicating the temperature dependence of the electronic conduction in the nematic phase by a simple scheme based on the hopping conduction in the Gay-Berne fluid. We found that the dynamic variation of the disorder plays an important role in the temperature dependence of the mobility in the nematic phase.

[1] H. Iino, J. Hanna, R. J. Bushby, B. Movaghar, B. J. Whitaker, and M. J. Cook, Appl. Phys. Lett. **87**, 132102 (2005).
[2] M. Funahashi and J. Hanna, Adv. Mater. (Weinheim, Ger.) **17**, 594 (2005).
[3] Z. An, J. Yu, S. C. Jones, S. Barlow, S. Yoo, B. Domercq, P. Prins, L. D. A. Siebbeles, B. Kippelen, and S. R. Marder, Adv. Mater. (Weinheim, Ger.) **17**, 2580 (2005).
[4] M. Funahashi and N. Tamaoki, ChemPhysChem **7**, 1193 (2006).
[5] M. Funahashi and N. Tamaoki, Chem. Mater. **19**, 608 (2007).
[6] K. L. Woon, M. P. Aldred, P. Vlachos, G. H. Mehl, T. Stirner, S. M. Kelly, and M. O'Neill, Chem. Mater. **18**, 2311 (2006).
[7] H. Bässler, Phys. Status Solidi B **175**, 15 (1993).
[8] P. M. Borsenberger and J. J. Fitzgerald, J. Phys. Chem. **97**, 4815 (1993).
[9] D. H. Dunlap, P. E. Parris, and V. M. Kenkre, Phys. Rev. Lett. **77**, 542 (1996).
[10] S. V. Novikov, D. H. Dunlap, V. M. Kenkre, P. E. Parris, and A. V. Vannikov, Phys. Rev. Lett. **81**, 4472 (1998).
[11] T. Kreouzis, K. J. Donovan, N. Boden, R. J. Bushby, O. R. Lozman, and Q. Liu, J. Chem. Phys. **114**, 1797 (2001).
[12] A. Ohno and J. Hanna, Appl. Phys. Lett. **82**, 751 (2003).
[13] M. J. Cook and M. R. Wilson, Mol. Cryst. Liq. Cryst. Sci. Technol., Sect. A **363**, 181 (2001).
[14] R. Berardi, L. Muccioli, and C. Zannoni, ChemPhysChem **5**, 104 (2004).
[15] J. G. Gay and B. J. Berne, J. Chem. Phys. **74**, 3316 (1971).
[16] L. F. Rull, Physica A **220**, 113 (1995).
[17] P. J. Camp and M. P. Allen, Physica A **229**, 410 (1996).
[18] R. Berardi and C. Zannoni, J. Chem. Phys. **113**, 5971 (2000).
[19] D. Wolf, P. Keblinski, S. R. Phillpot, and J. Eggebrecht, J. Chem. Phys. **110**, 8254 (1999).
[20] C. J. Fennell and J. D. Gezelter, J. Chem. Phys. **124**, 234104 (2006).
[21] S. Naemura and A. Sawada, Mol. Cryst. Liq. Cryst. **400**, 79 (2003).
[22] A. Sawada and S. Naemura, Jpn. J. Appl. Phys., Part 2 **41**, L195 (2002).